JOURNAL OF MATERIALS SCIENCE 31 (1996) 6171–6175

Source-material dependent growth limitations in unseeded dissociative sublimation of ZnSe

D. SICHE, H. HARTMANN
Institut für Kristallzüchtung im Forschungsverbund Berlin e.V. Rudower Chaussee 6, D-12489 Berlin, Germany

It has been found that besides temperature conditions, source-material composition (phase purity, impurity concentration and non-stoichiometry) dominates the quality of ZnSe crystals due to mass transport limitations and fluctuations. Therefore, without definite pretreatment, commercially supplied ZnSe source material is unsuitable for the physical vapour growth of ZnSe in closed systems. In this work the results of various characterization methods have been closely related to the optimal source preparation. For characterization of the non-stoichiometry of crystals, a qualitative relation between colour and zinc vacancy concentration has been established.

1. Introduction

Most progress in the development of blue–green light-emitting diodes has been based on ZnSe heteroepitaxy [1]. Because of the limitation of device lifetime, caused by defects arising from the hetero-interface [2], homoepitaxy substrates are of growing interest. Such substrates must be cut from high-quality bulk ZnSe crystals. Prerequisites for optimum homoepitaxy are: large single-crystalline area, no twinning, dislocation densities in the range 10^4–10^3 cm^{-2}, and (1 0 0) orientation with a high surface finish. Concerning these optimal properties, in agreement with the results of Eagle Picher [3] the best results are obtained for ZnSe crystals grown by the vapour-phase methods, especially physical vapour growth (PVT). In closed systems, mass transport rates and crystalline perfection were found to be strongly dependent on source-material composition. In our laboratory source materials have been characterized in terms of phase purity, chemical purity and stoichiometry. The grown crystals have been investigated for their non-stoichiometry-dependent colour (Table I) and their mass-transport related morphological and defect structure. Initial results and evidence for the p_{Zn}–T phase diagram [10] were published elsewhere [11]. In this context, the most difficult problem is the lack of quantitative analysis of non-stoichiometry, because the sensitivity of the usual methods is poor.

2. Source materials

For closed growth systems, the composition of the source material dominates the reproducibility of crystal growth. Precise control of source material composition is required for well-defined transport and growth rates. Some commercial ZnSe charges, delivered in powder form (size of grains 3–50 μm) or as pieces 3–6 mm diameter, were used. Without pretreatment, none of this material was suitable for growth experiments. Thus it was important to develop source-preparation techniques independently of starting material charges.

It was found, that unreacted elemental phases and volatile impurities decrease source sublimation and are responsible for a dramatic lowering of transport rates during the growth process. Deviations from stoichiometry have the same effect, but less strongly.

2.1. Phase purity

Excess elemental phases in the sources have been analysed for zinc and selenium excess.

(a) Zn excess. Yellow–green coloured powder was fired under crystal growth conditions for several days. Zinc excess, up to 2 at %, condensed in the cooler tip of the ampoule; the sinter process was incomplete and no ZnSe transport took place.

(b) Se excess. Orange-coloured powder was oxidized in streaming oxygen, for $x \sim 0.5$ corresponding to the reaction

$$2Zn_{1-x}Se_x(s) + (1 + x)\,O_x(g) = 2(1 - x)ZnO(s) + 2xSeO_x(g) \quad (1)$$

Selenium excess up to 0.2 at % was identified by gravimetry.

By each method, only one kind of excess component can be identified. It was expected that the other component may exist in unreacted elemental form at the same time. Firing the powder at 700 °C for several hours in a dynamic vacuum has been shown to purify the source material very effectively by evaporation of elemental components.

0022–2461

2.2. Impurities

The ZnSe powders were of a 99·999% purity. The concentrations of the main impurities as determined by the supplier (copper and iron at 5×10^{-4} mass %, nickel and cobalt at 5×10^{-5} mass %) yields native defect concentrations (estimated from the phase diagram) of 10^{16} cm^{-3}. There was no information about the carbon concentration, which was found by mass spectroscopy to be one order of magnitude higher. The highest concentrations of carbon were detected in pellets produced by chemical vapour deposition (CVD) on carbon glass substrates.

Quantitative analysis of 100 mg samples was done by means of inductively coupled plasma–open emission spectroscopy (ICP–OES). This method attains parts per million-level sensitivity for metals. Elements with atomic numbers lower than 11, especially carbon and oxygen, are not detectable. Results are listed in Table II.

Secondary ion mass spectroscopy (SIMS) was used for qualitative impurity analysis with lateral resolution of some micrometres and, in conjunction with sputtering a depth resolution in the submicrometre range (Table III). Surface contamination and impurity distributions (e.g. at grain boundaries in sintered source material residues) were analysed. In the bulk, no impurities were detected by SIMS (e.g. at a depth of 0.05 μm, no carbon and at 0.7 μm no silicon was found).

2.3. Stoichiometry

The stability range of the solid ZnSe phase in diagram Fig. 1 is extremely small and yields native defects (net vacancy concentrations) of 10^{16} cm^{-3} maximum, this

TABLE I Published colours for various $Zn_{1-y}Se_{1+y}$ preparation methods. SPVT, seeded vapour phase transport; SPGT, solid phase growth technique; IBD, ion beam deposition; EBE, electron beam evaporation; PB, phase boundary

Colour	Published techniques and present results			Present sample	y
530 nm green	Polycryst./Se – annealed 800 °C (SPGT) [5]	Polycryst./PB concave PVT [6]	Se – annealed 30 d, 900 °C p-type [8]	283b	> 0
Yellow–green	Polycryst./Se – annealed (PVT)	Polycryst./$p_{Zn,min}$ in the gas phase PB convex [9]			$\geqslant 0$
585 nm yellow	Polycryst./Zn – annealed 800 °C (SPGT) [5]	Single cryst./ PB concave PVT [6]	Zn – annealed 30d, 900 °C n-type [8]	285:Zn	$\leqslant 0$
Pale yellow	Single cryst. stoichiometric (SPVT) [4]			283a	$\cong 0$
Yellow–orange	Multicrystalline near stoichiometry (SPGT) [5]	Polycryst./[7] layer near stoichiometric (IBD)	Multicrystalline Zn – annealed PVT, near stoichiometry		≈ 0
605 nm orange	Polycryst./ PB convex (PVT) [6]	Polycryst./Se – annealed (PVT)			> 0
Orange–red	Polycryst./ PB convex (PVT) [6]			285	> 0
640 nm red	Polycryst./Ga-doped (SPVT) [4]			255	$\geqslant 0$
Red–brown	Polycryst./ [7] (EBE) layer non-stoichiometric				$\gg 0$

TABLE II Impurity concentration from ICP–OES analysis (p.p.m.)

Sample[a]	Cu	Fe	Cr	Si	Al	Cd	Ca
273b	1.50	< 0.5	< 0.6	< 3	< 0.3		
329	< 0.7	1.60	0.14	< 8.6	0.60	0.60	0.90
329R1	2.10	0.60	0.08	< 5.3	0.80	0.60	0.80
355	0.73	< 0.2	< 0.3	< 1.4	< 0.1		
355R	0.62	0.24	< 0.3	< 1.4	< 0.1		
MP-US	0.78	< 0.2	< 0.3	< 1.2	< 0.1		
MP-R	0.29	0.20	< 0.3	< 1.2	0.15		

[a] Sample name: R, source residue; MP, pellets; US, sublimated.

TABLE III Qualitative surface impurity concentration from SIMS analysis (counts)

	Source							
	O_2				Cs			
Sample[a]	Cu	Fe	Cr	Si	S	C	O_2	Al
273b	30	200	30	200	25	30000	200	500
277	50				200	100	40000	
329	3000	20	10	8000	3000	60	60	
329R1	20	10			1000	5		4
329R2	10	100	20		300	3000	25	30

[a] Sample name: R, source residue.

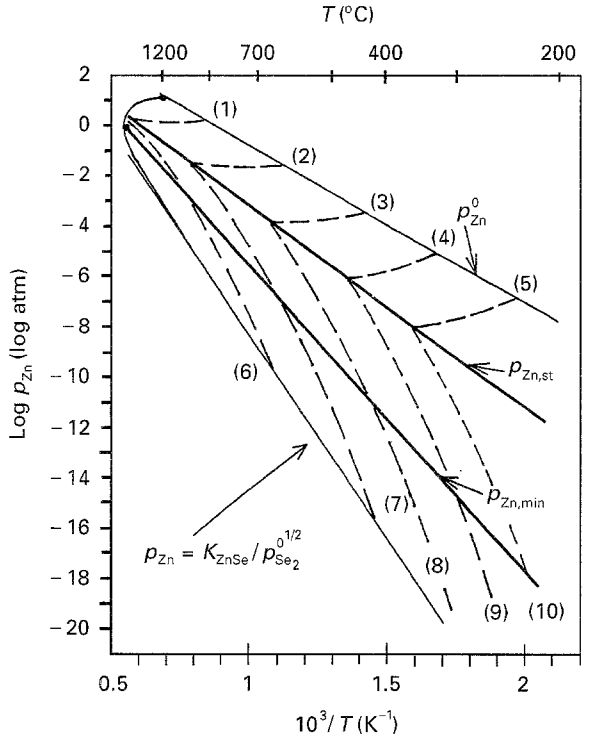

Figure 1 Homogeneity range of ZnSe in p–T coordinates. (– – –) Equal composition and refer to the following net vacancy concentrations (cm^{-3}): $[V_{Se}]$–$[V_{Zn}]$ = (1) 10^{16}; (2) 10^{14}; (3) 10^{12}; (4) 10^{10}; (5) 10^8; (6) $[V_{Zn}]$–$[V_{Se}] = 10^{16}$; (7) 10^{14}; (8) 10^{12}; (9) 10^{10}; (10) 10^8. $p_{Zn,St}$ is the zinc partial pressure over the stoichiometric compound [10].

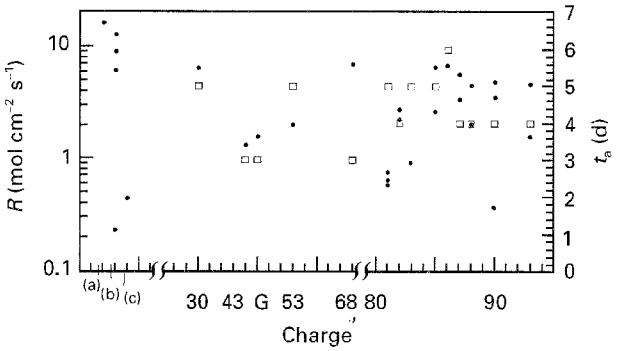

Figure 2 (●) Mass transport rates, R, and (□) annealing times, t_a, for different source-material charges: (a) sublimated, p_{min}; (b) CVD, near stoichiometric; (c) sublimated, selenium excess; below 81, p_{min} annealed; above 81, stoichiometric annealed; G mixture of 72, 73 and 80.

means 10^{-4} at %. Until now no quantitative method has been available for the detection of such small changes in matrix concentration. Previously, it has been shown, that in closed systems the most important prerequisite for the growth of stoichiometric crystals is a definite zinc excess in homogeneous source material [11], obtained by long-term annealing of powder at 900 °C under controlled zinc partial pressure. In this, the temperature of the zinc reservoir, T_{Zn}, is related to p^0_{Zn} of stoichiometric ZnSe at the growth temperature, T_g (Fig. 1; e.g. $T_g = 1150$ °C, $T_{Zn} = 727$ °C and $p^0_{Zn} = 0.11$ atm). Because of the lack of adequate self-diffusion data, the annealing time was estimated using the average diameter of powder grains (7 μm) and diffusion coefficients published elsewhere [12]. Furthermore, colour is a reliable qualitative indicator for the non-stoichiometry of grown crystals, but it gives no information on homogeneity in annealed powders. No change of mass transport rates with powder annealing times longer than 4 days was found (Fig. 2). Therefore, it may be inferred that our annealing procedure gives a homogeneous powder material.

Sublimation at 1000 °C is a very effective purification step with regard to unreacted components and volatile impurities. Some hundreds of grams of ZnSe have been transported under dynamic vacuum along a temperature gradient of nearly 5 K cm^{-1} in a horizontal quartz tube. From the phase diagram (Fig. 1), selenium-rich material with a composition related to $p_{Zn,min}$ was expected to condense first (at 860 °C). Because of the higher selenium partial pressure, the selenium excess in deposited ZnSe should increase with decreasing temperature. This trend is experimentally supported by the observation of a variation in colour over the tube length, going from yellow through orange to dark red. Additionally, increasing selenium excess was detected by means of chemical analysis (complexometric titration, CT). The experimental results from Chen *et al.* [13] may be interpreted in the same way.

To obtain homogeneous source material, the sublimated and compositionally graded material must be annealed and equilibrated under the crystal growth conditions.

3. Mass transport and crystal quality

For all growth experiments, mass-transport rates were measured and at the same time the perfection of the crystals was analysed. To investigate the influence of source material properties on crystal quality, temperature conditions must be known. In our experiments the source evaporation temperature was in the range $T_s = 1100$–$1200\,^{\circ}C$ and the temperature difference between the source and the ampoule tip was $\Delta T = 10$–80 K. For high supersaturations ($\Delta T > 25$ K) polycrystalline growth was observed. There is a weak dependence of transport rates on temperature as expressed by Faktor and Garret [14] in

$$J_{ZnSe} = \frac{2D_{AB}p}{3RT_{av}l} \ln\left(\frac{3p^0_{Zn} - 2p}{3p^1_{Zn} - 2p}\right) \qquad (2)$$

(where D_{AB} is the binary diffusion coefficient, p the total pressure at average ampoule temperature T_{av}, p_{Zn} the zinc partial pressure at the growing crystal interface (0) and at the source (1), and R the gas constant), where the argument of the ln-function with $\Delta T \geqslant 10$ K (responsible for $\Delta p_{Zn} = p^1_{Zn} - p^0_{Zn}$) enables only small changes in mass transport. At temperatures below 1050 °C, the growth rates decrease considerably due to kinetic limitations at the growing interface. In the interest of the stability of silica ampoules and low vacancy levels in the crystals with growth times of a maximum of 14 days, an optimum growth temperature of 1100 °C was established.

Under these conditions, changes in transport rates and defect density in the crystals were found to depend on source material composition and, in homogeneous material especially, on non-stoichiometry (Fig. 2).

Theoretical studies on the influence of non-stoichiometry on transport and growth rates have been done by Faktor *et al.* [15] and Ballentyne *et al.* [16]. Experimental results have been published elsewhere [11]. The main conclusion was that the transport rates and the critical rates for stable growth decrease with increasing excess of one component in the gas phase.

4. Characterization of crystals

The quality of the crystals was determined in terms of morphological stability and chemical homogeneity. The crystals were characterized by optical microscopy with respect to facets, twins, macro steps and etch-pit density. For prepared slices, surfaces were analysed by double-crystal X-ray diffraction rocking curves with best full width at half maximum (FWHM) values of about 20–30 arc sec in nearly stoichiometric material (sample 283a).

The previously described variation in colour was used for qualitative characterization of non-stoichiometry. Attempts were made to quantify this effect by room-temperature transmission measurements. A small red shift and a lower slope of the absorption edge were induced by increasing selenium excess (increasing zinc vacancy concentration $[V_{Zn}]$). However, calibration experiments were not successful (Table IV). The results of positron annihilation (PA) correlate with the specific resistivities, ρ, and infrared absorption of samples. Because the lowest single vacancy concentrations detectable by PA were in the 10^{15} cm^{-3} range, the results can be explained only by the presence of V_{Zn} clusters with decreased electrical activity. For as grown-samples $\rho \approx [V_{Zn}]^{-1}$ was found, but in sample 255 the resistivity was lowered by linear defects. In the zinc-extracted sample, donors are responsible for low ρ. Infrared absorption coefficients were measured calometrically by ballistic evaluation of sample heating above room temperature after absorption of a CO_2-laser pulse. This depends on the concentration of all point defects and becomes a minimum for the stoichiometric sample 283a.

ICP–OES, SIMS, CT, photoluminescence (PL), cathodoluminescence (CL) and electron paramagnetic resonance (EPR) have been used for investigation of crystals to obtain information about purity and chemical homogeneity. A zinc accumulation in crystals was detected by CT (crystal 320a with 50.17 ± 0.05 at % Zn and the residue of 320a with 49.83 ± 0.05 at % Zn). ICP–OES results are listed in Table II and there is evidence of a high purity level, but of no additional purification by vapour growth.

Qualitative SIMS results are listed in Table III. In some cases, high impurity levels were detected on crystal facets and on prepared surfaces. In less than 1 μm depth these concentrations fall below the detection limit of 5–10 counts. The presence of silicon, carbon, aluminium and oxygen is due to surface preparation (organic solvents, polishing agents) and the iron, chromium and copper contamination may be caused by sample handling.

TABLE IV Concentration of zinc vacancies from positron annihilation spectroscopy (PA), specific electrical resistivity, ρ, and infrared absorption coefficient, α

	Sample				
	255	283a	283b	285	285:Zn
Colour	Red	Pale yellow	Green	Orange–red	Yellow
τ_a (ps)[a]	246.4	245.8	240.9	240	242.4
$[V_{Zn}]$ (cm^{-3})[b]	1.3×10^{16}	1.1×10^{16}	1.7×10^{15}	$< 10^{15}$	4.5×10^{15}
$\rho_{300\,K}$ (Ω cm)	3.0×10^{8}	6.5×10^{8}	4.4×10^{9}	$> 10^{10}$	10^2–10^3
$\alpha_{10.6\,\mu m,RT}$ (%)	1.09	0.17	0.97	–	–

[a] τ_a average positron life time (measured).

[b] $[V_{Zn}] = \kappa/\mu$ with $\kappa = (\tau_a - \tau_b)/\tau_b(\tau_2 - \tau_a)$ ($\tau_2 = 240$ ps in ideal crystal volume (bulk), $\tau_2 = 340$ ps for maximum concentration of V_{Zn}) and the specific positron capture rate $\mu = 2.3 \times 10^{-8}$ cm^3 s^{-1}.

TABLE V Point defect identification from EPR analysis

Sample	Colour	Source material caused non-stoichiometry	Dark	Illuminated	Comment
289b	Yellow–orange	Near stoichiometry small Se excess	No spectrum	V_{Zn} (A-centre: V_{Zn}–Cl) and V_{Se} (or enclosed $3d^9$-ion e.g. Cu)	Concentrations in 10^{15}–10^{16} cm^{-3} range, strong compensation
243b	Green	Se excess	No vacancies, Fe^{3+}–Cu-pair on Zn site and Fe^{3+}–X		X, because no hyperfine structure was observed
261a	Red	Strong Se excess	Fe^{3+}–X	Fe^{3+}–X and V_{Zn}	Probably A-centre

The intensity of several lines in the PL spectra at low temperatures is the most characteristic feature for qualitative analysis of defect structure in crystals and prepared substrates. In particular, the I^1_{deep} line for V_{Zn}, the donor–acceptor pair spectra (DA) for impurities, the X line for free excitons and thus a low point-defect concentration and the Y line for a high dislocation density, have been used. In highly non-stoichiometric samples, copper green, copper red and self-activated luminescence (SA), which is caused by V_{Zn}–X complexes, was observed.

By means of the CL mode of a scanning electron microscope, analogous results have been obtained, but with better local resolution.

Initial results of EPR measurements (listed in Table V) also support our model that there is a relation between crystal colour and $[V_{Zn}]$. Other defects like V_{Se} and pair defects were found by this method if the conversion in the paramagnetic condition was possible. The main experimental problem was to obtain EPR spectra which could be unambiguously interpreted. For this reason, single-crystalline rectangular parallelepipeds were cut with dimensions 3 mm × 3 mm × 5 mm and a (1 1 0) orientation of the 3 mm × 3 mm front side. Non-stoichiometric crystals from unseeded PVT were often polycrystalline and then optimal sample preparation was more difficult. Otherwise, there is a high potential for investigation of seed-grown crystals.

5. Conclusion

In closed vapour-growth systems, the crystal quality is dominated by the source-material composition. Several methods have been used for characterization of source material and crystals defect structure, which are related by mass transport and growth rates. Without an effective treatment of commercially supplied source material, no optimal crystal growth by PVT is possible. For deviation from stoichiometry, no quantitative measure was found, but non-stoichiometry realized by vacancies is correlated to colour of crystals and is qualitatively evident by vacancy-sensitive methods.

Acknowledgements

We are indebted to Dr R. Krause-Rehberg, PA Laboratory, Department of Physics, Martin Luther University, Halle, Dr M. Wienecke, Institute of Materials Science, Department of Physics, Humboldt University, Berlin, and R. Krupka, Institute for Beam Tools, University of Stuttgart, for τ_a, $\rho_{300\,K}$ and $\alpha_{10.6\,\mu m,RT}$, measurements of Table IV, and Dr J. Kreißl, EPR Laboratory, Institute of Solid State Physics, Technical University, Berlin, for measurements in Table V. This work was supported by the Deutsche Forschungsgemeinschaft.

References

1. M. A. HAASE, J. QIU, J. M. DE PUYDT and H. CHENG, *Appl. Phys. Lett.* **59** (1991) 1272.
2. G. C. HUA, N. OTSUKA, D. C. GRILLO, Y. FAN, J. HAN, M. D. RINGLE, R. L. GUNSHOR, M. HOVINEN and A. V. NURMIKKO, *ibid.* **65** (1994) 1331.
3. W. C. HARSCH, private communication (1994).
4. J. M. HAYS, W. SHAN, X. H. YANG, J. J. SONG and E. CANTWELL, *Semicond. Sci. Technol.* **7** (1992) 1408.
5. K. TERASHIMA, M. KAWACHI and M. TAKENA, *J. Crystal Growth* **104** (1990) 468.
6. F. ALLEGRETTI, A. CARRARA and S. PISSINI, *J. Cryst. Growth* **128** (1993) 646.
7. A. KUROYANAGI, *J. Appl. Phys.* **68** (1990) 5568.
8. M. WIENECKE, Humboldt-University, Berlin, private communication (1993).
9. J. R. CUTTER and J. WOODS, *J. Crystal Growth* **47** (1979) 405.
10. H. HARTMANN, R. MACH and B. SELLE, "Wide gap II–VI compounds as electronic materials", "Current Topics in Materials Science", Vol. 9, edited by E. Kaldis (North-Holland, Amsterdam, 1982).
11. H. HARTMANN and D. SICHE, *J. Crystal Growth* **138** (1994) 260.
12. M. M. HENNEBERG and D. A. STEVENSON, *Phys. Status Solidi (b)* **48** (1971) 255.
13. K.-T. CHEN, M. A. GEORGE, Y. ZHANG, A. BURGER, C.-M. SU, Y.-G. SHA, D. C. GILLIES and S. L. LEHOCZKY, *J. Crystal Growth* **147** (1995) 292.
14. M. M. FAKTOR and I. GARRETT, "Growth of Crystals from the Vapour" (Chapman and Hall, London, 1974).
15. M. M. FAKTOR, J. GARRETT and R. HECKINGBOTTOM, *J. Crystal Growth* **9** (1971) 3.
16. D. W. G. BALLENTYNE, S. WETWATANA and E. A. D. WHITE, *ibid.* **7** (1970) 79.

Received 20 November 1995
and accepted 5 July 1996